



Synthesis and photovoltaic properties of organic sensitizers containing electron-deficient and electron-rich fused thiophene for dye-sensitized solar cells

Xiaobing Cheng, Mao Liang*, Siyuan Sun, Yongbo Shi, Zijian Ma, Zhe Sun, Song Xue*

Department of Applied Chemistry, Tianjin University of Technology, Tianjin 300384, PR China

ARTICLE INFO

Article history:

Received 4 March 2012

Received in revised form 15 April 2012

Accepted 28 April 2012

Available online 3 May 2012

Keywords:

Dye-sensitized solar cell

Organic sensitizers

Electron-deficient fused thiophene

ABSTRACT

Diverse fused thiophenes with electron-rich and electron-deficient blocks have been synthesized and employed as the π -conjugated spacers of organic dyes for the dye-sensitized solar cells (DSSCs). The effects of these fused thiophenes were investigated by their absorption spectra, electrochemical and photovoltaic properties. For a typical device a maximum power conversion efficiency of 6.11% was obtained under simulated AM 1.5 irradiation (100 mW cm^{-2}): a short-circuit current (J_{SC}) of 14.47 mA cm^{-2} , an open-circuit voltage (V_{OC}) of 670 mV, and a fill factor (FF) of 0.63.

© 2012 Elsevier Ltd. All rights reserved.

1. Introduction

There has been considerable interest for developing cheap and easily accessible renewable energy sources due to increasing energy demands and concerns about global warming. Compared to traditional silicon-based solar cells, dye-sensitized solar cells (DSSCs) are viewed as promising candidate for renewable clean energy sources in virtue of their low manufacturing cost and impressive photovoltaic performance.¹ To achieve high solar power conversion efficiency, great research efforts are focused on designing and synthesizing new photosensitizers: Ru-based complexes² and organic sensitizers.³ The former holds the record of validated efficiency of over 11%.^{2b} Organic sensitizers with robust availability, ease of structural tunability, and generally high molar extinction coefficients, have emerged as a competitive alternative to the Ru-based counterpart.^{4–24} So far, the metal-free organic sensitizers have gained promising solar energy-to-electricity conversion efficiencies (η) comparable to Ru-based complexes.^{25–28}

Aside from electron donor (D) and acceptor (A) in a typical D- π -A system, the conjugated bridging segment (π) is widely recognized as its significance for performance control of DSSCs. Introduction of fused ring building blocks^{20,26,29–33} involved of rigid thieno[3,2-*b*]thiophene (TT), dithieno[3,2-*b*:2',3'-*d*]thiophene (DTT), cyclopentadithiophene, dihexyl-substituted dithienosilole, and benzo [1,2-*b*:4,5-*b'*]dithiophene in the π -spacer is proved to be effective strategies for enhancing the light-harvesting capacity, leading to

impressive performances under standard global air mass 1.5 (AM 1.5G) illumination. The majority of research on fused ring building blocks has focused on electron-rich fused thiophene; however, electron-deficient fused thiophene has not yet to be explored for organic dyes. It is known that electron-deficient materials were successfully in application of bulk heterojunction organic photovoltaic cells (OPVs).^{34–36} It can be expected that developing of new type fused ring building blocks may lead to synthesis of interesting photosensitizers with tailor-made photophysical, electrochemical, and other properties to fulfill those requirements for high performance of DSSCs.

Herein, we report the design, syntheses, and photovoltaic properties of a series of new triphenylamine dyes (**XS35–38**) incorporating electron-rich and electron-deficient fused thiophene units. For obtaining high photovoltaic performance, binary spacers of a combination of EDOT and different fused thiophenes were introduced. In the case of **XS36** and **XS38**, electron-rich fused thiophene units, DTT, and 3-methylthieno[3,2-*b*]thiophene (MTT) are introduced, respectively. Meanwhile, electron-deficient fused thiophene units, dithieno[3,2-*b*:2',3'-*d*]thiophene-4,4-dioxide (DTTO) and 3-methylthieno[3,2-*b*]thiophene-4,4-dioxide (MTTO) are introduced into the structure of **XS35** and **XS37**, respectively. These designed dyes allow us to better understand the structure–property relationship of metal-free organic chromophores. Molecular structures of these two dyes are shown in Fig. 1.

2. Results and discussion

The synthetic routes of four organic dyes **XS35–38** are shown in Scheme 1. DTT³⁷ and MTT³⁸ units were prepared according to

* Corresponding authors. Tel.: +86 22 60214250; fax: +86 22 60214252; e-mail addresses: liangmao717@126.com (M. Liang), xuesong@ustc.edu.cn (S. Xue).

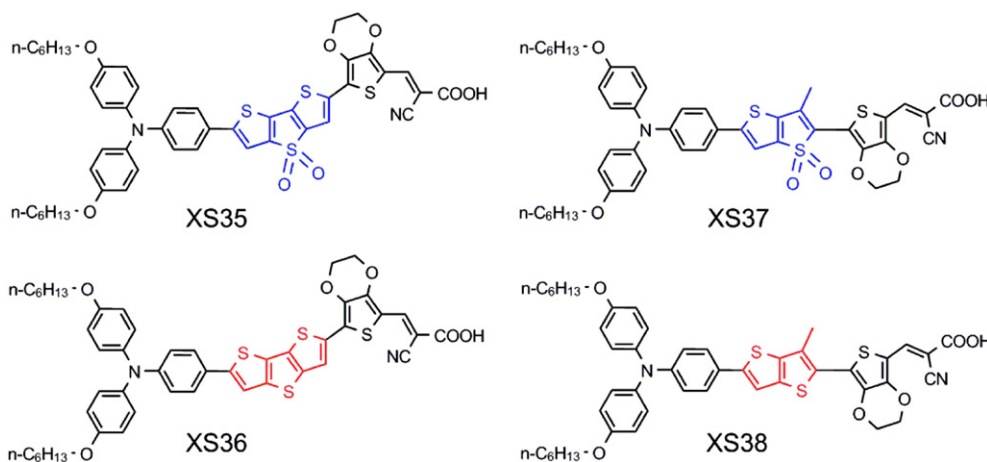


Fig. 1. Structure of dyes (XS35–38).

literature. DTTO and MTTO were obtained by using the methodology described by Matzger et al.³⁹ and Barbarella et al.,⁴⁰ respectively. XS35 was synthesized in six steps from the DTTO. The Stille coupling of compound **2** with 4-(hexyloxy)-*N*-(4-(hexyloxy)phenyl)-*N*-(4-(tributylstannyl)phenyl)aniline yielded compound **3**. Compound **4**, synthesized from bromination with *N*-bromosuccinimide (NBS) in DMF, was cross-coupled with tributyl(2,3-dihydrothieno[3,4-*b*][1,4]dioxin-5-yl)stannane to give compound **5**. Aldehyde **6** was synthesized from the reaction of **5** with POCl₃ and DMF through the Vilsmeier–Haack reaction. Then the target dye XS35 was obtained via Knoevenagel condensation reaction of the aldehyde **6** with cyanoacetic acid in the presence of a catalytic amount of piperidine. The synthetic routes for XS36–38 are similar to that of XS35. The intermediates **10**, **16**, and **20** were obtained through bromination, Suzuki coupling, and Vilsmeier–Haack reaction. Treatment of these intermediates with 4-(hexyloxy)-*N*-(4-(hexyloxy)phenyl)-*N*-(4-(tributylstannyl)phenyl)aniline through the Stille coupling reaction gave important intermediates of aldehydes **11**, **17**, and **21**, respectively. The Knoevenagel condensation of these aldehydes with cyanoacetic acid in the presence of piperidine in CH₃CN yielded organic sensitizers XS36–38.

2.1. Absorption spectra

The UV–vis and emission spectra of organic dyes in chloroform are displayed in Fig. 2. The four dyes have one intense visible absorption band centered about 500 nm corresponding to the intramolecular charge-transfer (ICT) band. The absorption peaks (λ_{max}) for XS35, XS36, XS37, and XS38 are located at 514, 497, 492, and 494 nm, respectively. Obviously, in the case of sensitizers containing the same donor and acceptor units, the ICT band is dependent upon the π -spacer units. The π -spacer effect on the absorption peak is distinct in these four dyes. The bathochromic shift by 17 nm was observed when replacing DTT unit (XS36) with DTTO unit (XS35) in the spacer moiety. This observation arising from introduction of deficient bridge has also been observed by other groups.^{25,41,42} However, such an effect is partially annihilated upon replacing MTTO unit with MTT unit for XS37. Under the same conditions, the XS37 sensitizer exhibits a slightly blue-shifted absorption band relative to XS38. This observation can be interpreted from molecular model studies. The structures of the dyes were analyzed using a B3LYP/6-31G(d) hybrid function for full geometrical optimization (Fig. 3). In the ground state, XS35, XS36, and XS38 possess a nearly co-planar conformation to achieve a maximal extent of π -delocalization. In the case of XS37, the torsion angle between MTTO and EDOT (-20.3°) is larger due to the steric hindrance of sulfonyl

and ethylenedioxy groups compared to the XS35, XS36, and XS38 counterpart, decreasing the electronic communication between donor and acceptor. The molar extinction coefficients of XS35–38 are 39×10^3 , 44×10^3 , 21×10^3 , and $37 \times 10^3 \text{ M}^{-1} \text{ cm}^{-1}$, respectively. XS37 exhibited the lowest absorptivity, reflecting the important role of molecular conformation.

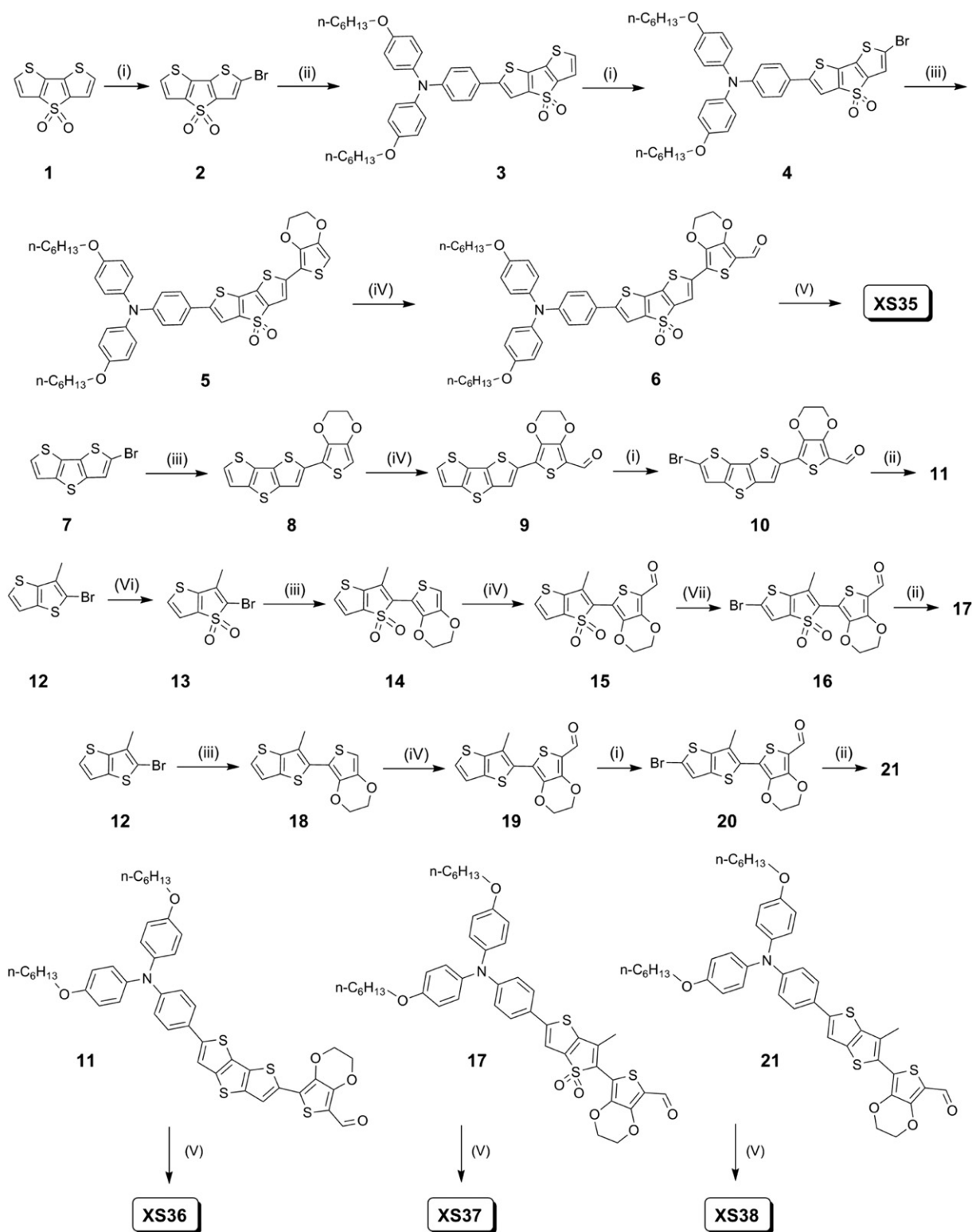
Upon adsorption onto TiO₂, XS35–38 show similar hypsochromic effect compared with that measured in solution (Fig. 4), which could be ascribed to a weaker electron-withdrawing capability of the carboxylate/titanium assembly than the carboxylic acid.⁴¹ When the four dyes are excited with visible light, they exhibit strong luminescence maxima at 550–750 nm (Fig. 2b).

2.2. Electrochemical properties

The first ground-state oxidation potentials (E_{D/D^+}), corresponding to the HOMO level of dyes, were measured by cyclic voltammetry (CV) with 0.1 M tetrabutylammonium perchlorate in acetonitrile solution and the results were summarized in Table 1. The LUMO levels of sensitizer were estimated by the values of E_{D/D^+} and the 0–0 band gaps. The latter is obtained by the intersection of absorption and emission spectra. As depicted in Fig. 5, introduction of different types of fused thiophene in the spacer can adjust the HOMO and the LUMO levels of these dyes. Positive shifts of the HOMO level (0.1 V) and the LUMO level (0.1 V) are observed for XS35 versus XS36. Also, this tendency holds for XS37 versus XS38. It is suggested that, compared to the electron-deficient thiophene, the electron-rich fused thiophene raises the oxidation potential of dye. The E_{D/D^+} values of XS35–38 within the range of 0.71–0.83 V versus NHE are more positive than the iodine redox potential (0.4 V vs NHE).⁴³ Thus, these oxidized dyes can be regenerated from the reduced species in the electrolyte to give an efficient charge separation. The excited state reduction potentials (E_{D^*/D^+}) of the four dyes (-1.32 to -1.43 V vs NHE) are much more negative than the conduction band of TiO₂ at approximately -0.5 V versus NHE, providing enough driving force for electron injection.^{16,44}

2.3. Computational analysis

To get further insight into the molecular structure and electron distribution of these dyes, we performed TDDFT excited states calculations at the B3LYP/6-31G(d) level in vacuo with the B3LYP/6-31G(d) optimized ground-state geometries with Gaussian 03,⁴⁵ given the negligible effect of solvation on the electronic structure. The first and second transitions of XS35–38 with oscillator strengths (f) above 0.5 are summarized in Table 2. There are three



Scheme 1. Synthesis and structures of organic dyes. Reagents: (i) NBS, DMF, rt; (ii) 4-(tributylstannyl)-*N,N*-bis(4-hexyloxy)phenyl)aniline, Pd(PPh₃)₄, *p*-xylene, reflux; (iii) 2-(tributylstannyl)-3,4-(ethylenedioxy)thiophene, Pd(PPh₃)₄, *p*-xylene, reflux; (iv) DMF/POCl₃, 0 °C/rt; (v) CNCH₂COOH, CH₃CN/CHCl₃, piperidine, reflux; (vi) *m*-CPBA, CH₂Cl₂, 0 °C/rt; (vii) Br₂, CH₂Cl₂, 0 °C/rt.

charge-transfer excitations: HOMO→LUMO, HOMO–1→LUMO, and HOMO→LUMO+1 (Fig. 6). The electron distribution of the HOMO–1, HOMO, and LUMO of XS35–38 are similar. HOMO–1 and HOMO are populated over the triphenylamine and electron-rich/electron-deficient fused thiophene units with considerable contribution from the former. LUMO is delocalized through the

fused thiophene units, EDOT and cyanoacrylic acid fragments with sizable contribution from the latter. The HOMO–LUMO excitation moves the electron distribution from the diphenylvinyl unit to the cyanoacrylic acid moiety, thus allowing an efficient photoinduced electron transfer from the dye to the TiO₂ electrode under light irradiation. This spatially directed separation of

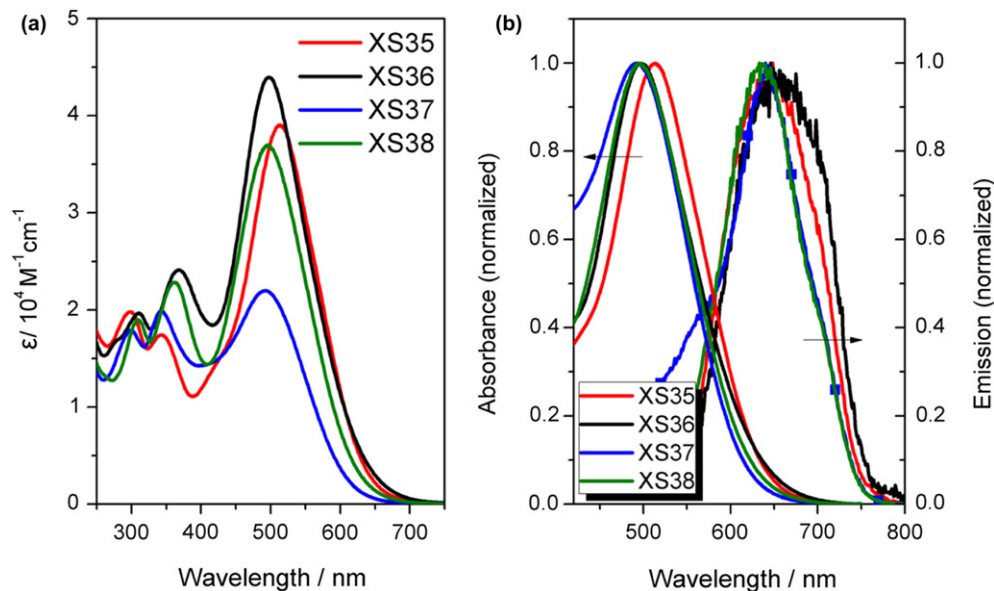


Fig. 2. Absorption (a) and normalized absorption and emission spectra (b) of dyes in chloroform (1×10^{-5} M).

HOMO and LUMO is an ideal condition for dye-sensitized solar cells. In the case of LUMO+1, electron rich or deficient linkers have an impact on the electron distribution. For **XS35** and **XS37**, the electron distribution of LUMO+1 is delocalized through the fused thiophene units, EDOT and cyanoacrylic acid fragments with considerable contribution from the former. It can be found that very small electron distribution is delocalized on the triphenylamine. For **XS36** and **XS38**, the electron distribution delocalized on the triphenylamine is large. Obviously, the spatially directed separation of HOMO and LUMO+1 of **XS35/XS37** are more completely than those of **XS36/XS38**. In view of this, deficient linker has a positive impact on the charge separation of D- π -A sensitizer.

2.4. Photovoltaic performance of DSSCs

The incident monochromatic photon-to-current conversion efficiency (IPCE) measurements of DSSCs based on **XS35–38** using the redox electrolyte consisting of 0.6 M DMPImI, 0.05 M I_2 , 0.1 M LiI, and 0.5 M TBP in acetonitrile are shown in Fig. 7. In agreement with the trend in absorption spectra, the IPCE spectra of **XS35**, **XS36**, and **XS38** exhibit higher peak values and longer wavelengths than that of **XS37**. It is notable that the onset of the IPCE data of **XS35**, **XS36**, and **XS38** is close to about 800 nm. The IPCE spectra of **XS35** and **XS38** exceed 70% in the visible spectral region from 430 to 620 nm, reaching their maximum of 82% and 90% around 480 nm, respectively, indicating highly efficient DSSCs performances. The IPCE

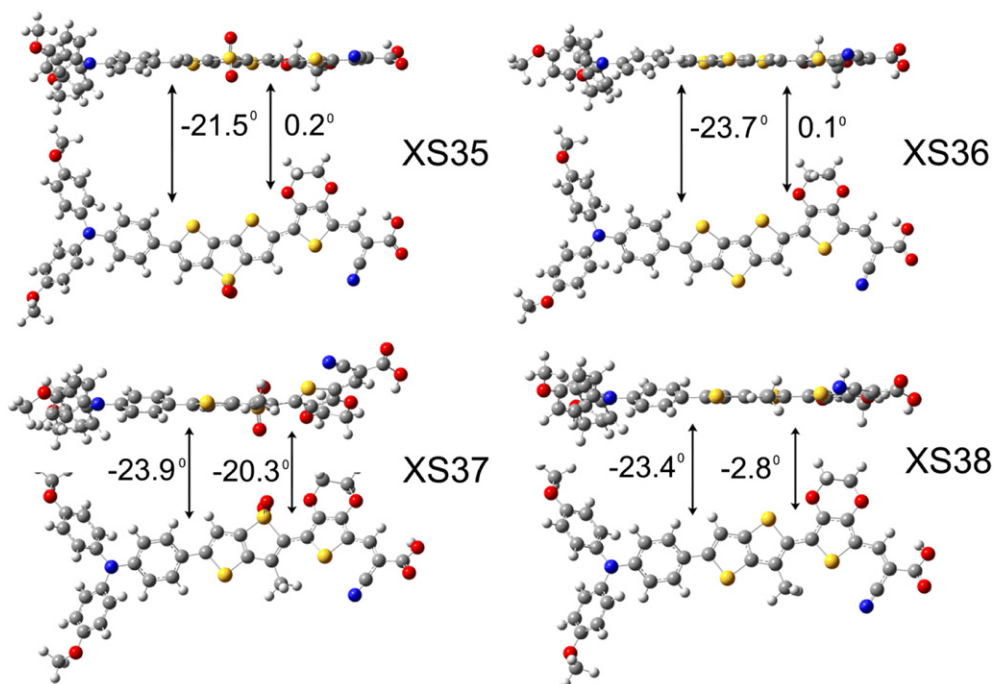


Fig. 3. The optimized structures of **XS35–38**.

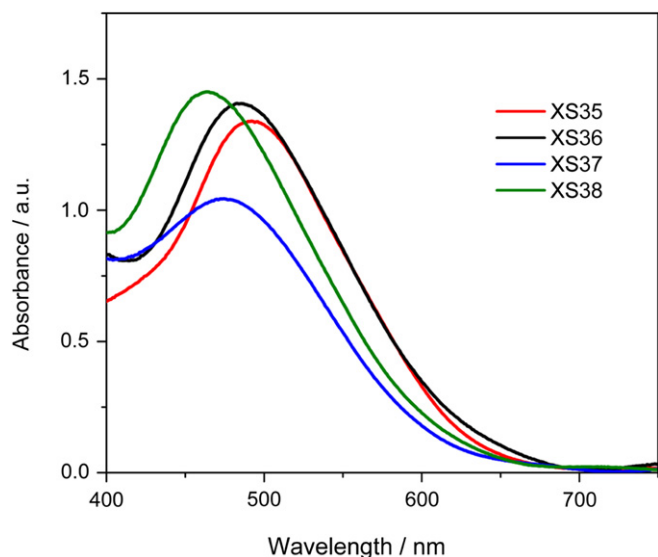


Fig. 4. Absorption spectra of dyes adsorbed on TiO₂ film (3 μm).

Table 1
Photophysical and electrochemical data for dyes

Dye	λ_{\max}^a /nm ($\epsilon/M^{-1} \text{cm}^{-1}$)	λ_{int}^b (nm)	$E_{D/D+}^c$ /V	$E_{D^+/D+}^d$ /V
XS35	514 (39,000)	582	0.81	-1.32
XS36	497 (44,000)	581	0.71	-1.42
XS37	492 (21,000)	565	0.82	-1.37
XS38	494 (37,000)	574	0.83	-1.43

^a The absorption spectra were measured in CHCl₃ solutions.

^b The intersect of the normalized absorption and the emission spectra.

^c $E_{D/D+}$ (vs NHE) was measured in acetonitrile.

^d $E_{D^+/D+}$ was calculated from $E_{D^+/D+} = E_{\text{ox}} - E_{0-0}$, $E_{0-0} = 1240/\lambda_{\text{int}}$.

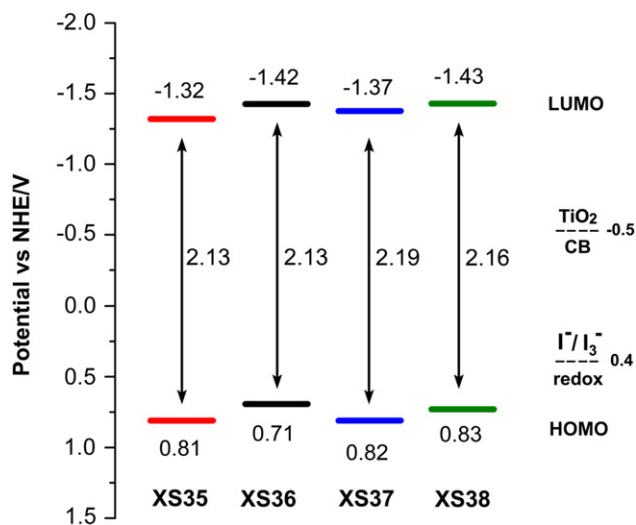


Fig. 5. Schematic energy levels of dyes based on absorption and electrochemical data.

performance of the DSSC with XS35 is broader and higher than those of XS36, which can be partially attributed to the broader light absorption. This phenomenon arises from the electron-deficient unit was also observed by other group.⁴² The IPCE performance of the DSSC based on XS38 is higher than that of XS36, despite with the larger molar extinction coefficient and more redshifted absorption. This is likely to be due to the higher surface coverages (Γ)

Table 2

Calculated details of electronic transitions with the relative oscillator strengths larger than 0.5 of the dyes

Dye	State	Calculated energy (eV, nm)	Oscillator strength (f)	Transition assignment ^a
XS35	1	1.79, 690	0.79	H → L (90%)
	2	2.45, 505	0.97	H-1 → L (58%) H → L+1 (30%)
XS36	1	1.90, 649	0.79	H → L (90%)
	2	2.54, 487	1.0	H-1 → L (80%) H → L+1 (4%)
XS37	1	1.79, 689	0.73	H → L (90%)
	2	2.51, 493	0.67	H-1 → L (74%) H → L+1 (8.8%)
XS38	1	2.01, 616	0.85	H → L (87%)
	2	2.67, 463	0.85	H-1 → L (79%) H → L+1 (4.5%)

^a H means HOMO, and L means LUMO.

of XS38. By comparing the absorbance change of a dye solution (300 μM) before and after dye up-taking with a titania film, the surface coverages (Γ) of XS35, XS36, XS37, and XS38 anchored on TiO₂ film were determined to be 2.7×10^{-7} , 2.3×10^{-7} , 3.0×10^{-7} , and 4.0×10^{-7} mol cm⁻², respectively. It can be found that, the surface coverages of XS37 and XS38 are higher than that of XS35 and XS36 due to their small molecular sizes, and thus the largest IPCEs of XS38 among the dyes can be partially ascribed to its simultaneously better light-harvesting ability and larger surface density on TiO₂. XS37 sensitized cell generates the lowest IPCE value among the three dyes, which may be due to its lower molar extinction coefficient and narrower absorption spectrum.

Photovoltaic tests were conducted to evaluate the potential of the XS35–38 dyes in DSSCs. The J - V curves of the DSSCs sensitized by the XS35–38 dyes are shown in Fig. 8. The detailed photovoltaic parameters are summarized in Table 3. Being consistent with the integrals of IPCEs over the standard AM 1.5G solar emission spectrum, XS38 yields the highest short-circuit photocurrent density (J_{SC}) amongst these four photosensitizers. With an open-circuit photovoltage (V_{OC}) of 670 mV and a fill factor (FF) of 0.63, an XS38-based cell exhibits a power conversion efficiency (η) of 6.11%. XS36-based cell presents lower η value than XS38-based counterpart, owing to relatively low J_{SC} and V_{OC} . Our photovoltaic characterization evidently demonstrates the superiority of MTT over DTT in binary spacers. Compared to XS36, XS35 with the bridge alteration from DTT to DTTO, not only evokes an enhancement of J_{SC} but concomitantly prompts a V_{OC} improvement, leading to higher conversion efficiency. In contrast, replacing MTT with MTTO does not generate similar effects, and XS37 presents the lowest η value primarily owing to relatively low photocurrents.

2.5. Electrochemical impedance spectroscopy

The V_{OC} values are in the sequence of XS37 < XS36 < XS35 < XS38. Through the introduction of electron-deficient fused thiophene (DTTO) into the binary spacer, one notes that the XS35-based cell gives an enhanced V_{OC} (20 mV) in contrast to the XS36-based cell. When the DTT unit is displaced by the MTT unit, the V_{OC} rises remarkably (i.e., V_{OC} of XS38 reaches 670 mV compared to that of XS36, 600 mV) under similar conditions, consequently leading to an increase of power conversion efficiency. The respectable increase of V_{OC} obtained by the delicate change in molecular structure is intriguing. To scrutinize the origin of the improvement in V_{OC} , measurement of the electrochemical impedance spectroscopy (EIS) is performed. The charge recombination resistance at the TiO₂/electrolyte interface (R_{CT}) was modeled from impedance spectroscopies as a function of applied potential bias. The charge recombination resistance is related to the charge recombination

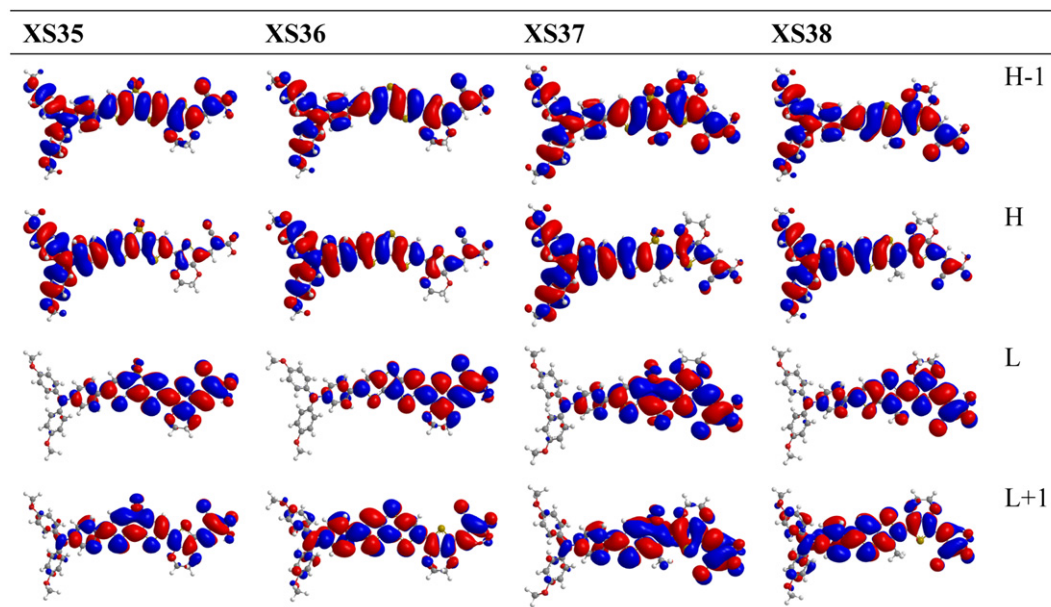


Fig. 6. Computed frontier orbitals of dyes. H means HOMO, and L means LUMO.

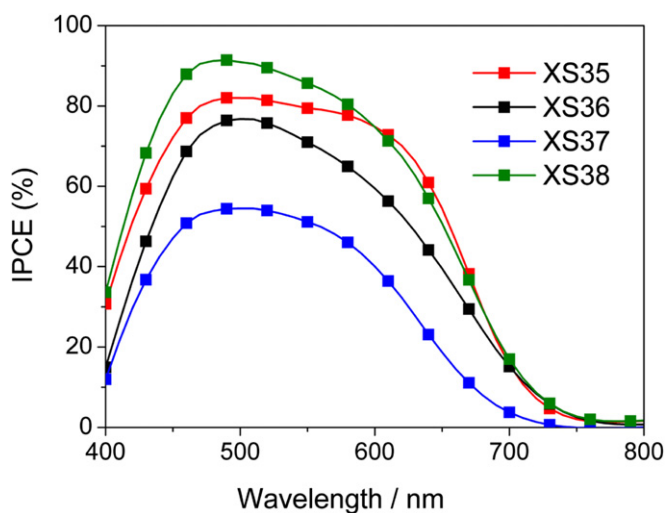


Fig. 7. IPCE spectra of DSSCs.

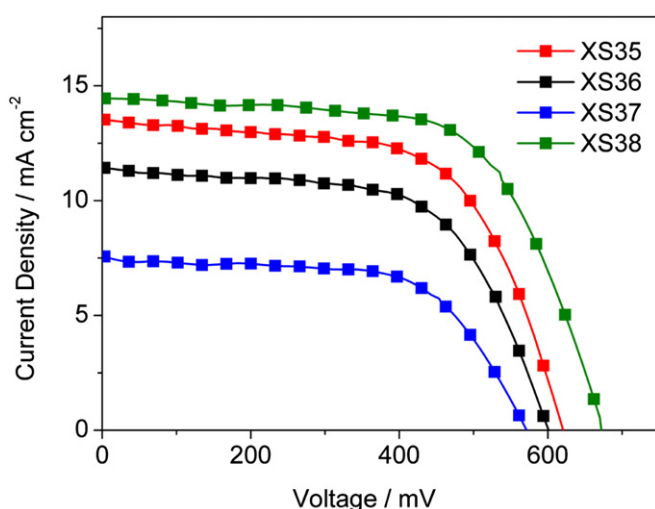


Fig. 8. J - V curves of DSSCs under AM 1.5G simulated solar light (100 mW cm^{-2}).

Table 3
Photovoltaic parameters for DSSCs^a

Dye	$J_{sc}/\text{mA cm}^{-2}$	V_{oc}/mV	FF	η (%)
XS35	13.52	620	0.62	5.19
XS36	11.42	600	0.61	4.18
XS37	7.56	567	0.63	2.70
XS38	14.47	670	0.63	6.11
N719	16.60	684	0.65	7.36

^a Performance of DSSCs measured in a 0.16 cm^2 working area. Irradiating light: AM 1.5G (100 mW cm^{-2}). The photovoltaic parameters are averaged values obtained from analysis of the J - V curves of three identical working electrodes for each device fabricated and characterized under the same experimental conditions.

rate, such that a smaller R_{CT} means the larger charge recombination rate. As presented in Fig. 9a, for the cobalt cells, the fitted R_{CT} increases in the order of $\text{XS37} < \text{XS36} < \text{XS35} < \text{XS38}$, indicating a same order of decreased charge recombination rate. By fitting the EIS curves, another important parameters for DSSCs, electron lifetime (τ), could be extracted from the C_{μ} and R_{CT} using $\tau = C_{\mu} R_{CT}$. The fitted τ increases in the order of $\text{XS37} < \text{XS36} < \text{XS35} < \text{XS38}$, indicating a sequence of lifetime increasing (Fig. 9b). These results are in agreement with the observed shift in the V_{oc} value under standard global AM 1.5 illumination. The longer lifetime of XS38 relative to XS36 is attributable to effective surface blocking as result of smaller molecular structure.^{20,46} The results from EIS also suggest that the two oxygen atoms of DTTO have an impact on the lifetime of dyes, which prevent hydrophilic I_3^- ions approaching the TiO_2 surface and thereby lead to suppressing charge recombination/dark current and lengthening electron lifetime.

For further support of the above viewpoint, the open-circuit voltage decay (OCVD) measurements were carried out. This technique measures the recombination lifetime of the injected electron with the photooxidized dye.⁴⁷ Fig. 10 shows the open-circuit potential decay transients of the DSSCs based on XS35–38. The voltage of solar cells decreased in the order of $\text{XS37} > \text{XS36} > \text{XS35} > \text{XS38}$. The results are consistent with measurements of EIS. High capability of XS38 to quickly inject the photogenerated electrons inside the TiO_2 network before exciton recombination induces high photovoltage, which tends to slowly decrease due to recombination losses.^{48,49}

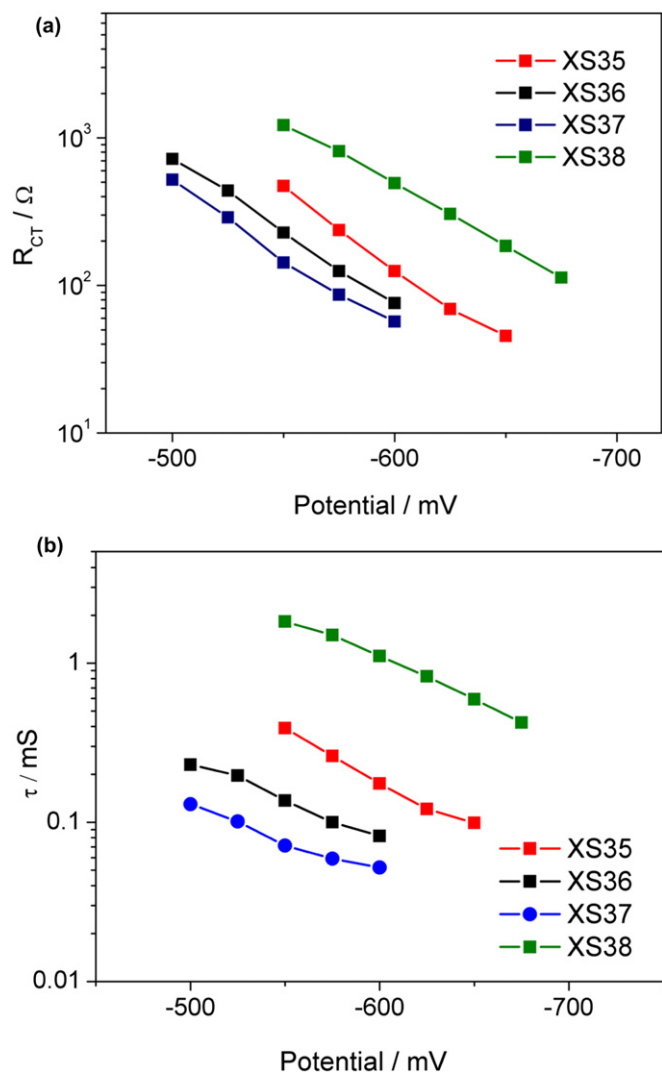


Fig. 9. Interfacial charge-transfer resistance R_{CT} (a) and electron lifetime τ fitted from impedance spectra under a series of applied potentials.

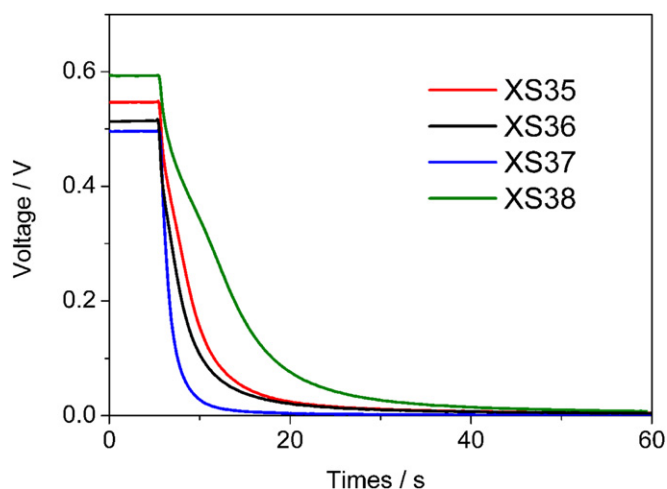


Fig. 10. Decay transients of the open-circuit potential.

3. Conclusions

In this paper, four new push–pull organic dyes incorporating electron-rich (DTT and MTT) and electron-deficient (DTTO and MTTO) fused thiophene as units of binary spacers have been synthesized, characterized, and used as sensitizers for DSSCs. The photovoltaic performance was shown to be quite sensitive to the fused thiophene unit of the spacer. MTT is superior to DTT when they are applied in binary spacer organic dyes. Compared to DTT, the introduction of DTTO into the binary spacer is advantageous to the light harvesting. But MTTO exhibits a slightly blue-shifted absorption relative to MTT due to the steric hindrance. The MTT-containing dye, XS38, showed the best photovoltaic performance with an overall conversion efficiency of 6.11% under standard global AM 1.5 solar light condition. The results reveal that development of new type fused thiophenes is an effective way for the development of sensitizers.

4. Experimental

4.1. Materials and instruments

The synthetic routes for dyes are shown in Scheme 1. *n*-Butyllithium was purchased from Alfa. *N,N*-Dimethylformamide was dried over and distilled from CaH_2 under an atmosphere of nitrogen. Phosphorus oxychloride was freshly distilled before use. Dichloromethane and chloroform were distilled from calcium hydride under nitrogen atmosphere. Titanium(IV) isopropoxide, *tert*-butylpyridine, and lithium iodide were purchased from Aldrich. All other solvents and chemicals used in this work were analytical grade and used without further purification.

^1H NMR and ^{13}C NMR spectra were recorded on a Bruker AM-300 or AM-400 spectrometer. Mass spectra were recorded on a LCQ AD (ThermoFinnigan, USA) mass spectrometer. The melting point was taken on an RY-1 thermometer and temperatures were uncorrected.

4.2. Photophysical and electrochemical measurements

The absorption spectra of the dyes either in solution or on the adsorbed TiO_2 films were measured by HITACHI U-3310 spectrophotometer. Adsorption of the dye on the TiO_2 surface was done by soaking the TiO_2 electrode in a dry chloroform solution of the dye (standard concentration 3×10^{-4} M) at room temperature for 24 h. Fluorescence measurement was carried with a HITACHI F-4500 fluorescence spectrophotometer. FT-IR spectra were obtained with a Bio-Rad FTS 135 FT-IR instrument.

Electrochemical measurements were performed at room temperature on a computer-controlled LK2005A electrochemical workstation with Pt-wires as working electrode and counter electrode, Ag/AgCl electrode as reference electrode at a scan rate of 100 mV s^{-1} . Tetrabutylammonium perchlorate (TBAP, 0.1 mol/L) and MeCN were used as supporting electrolyte and solvent, respectively. The measurements were calibrated using ferrocene as standard. The redox potential of ferrocene internal reference is taken as 0.63 V versus NHE.⁵⁰

4.3. Fabrication and characterization of DSSCs

The TiO_2 paste consisting of 18 wt % TiO_2 , 9 wt % ethyl cellulose, and 73 wt % terpineol was firstly prepared,⁵¹ which was printed on a conducting glass (Nippon Sheet Glass, Hyogo, Japan, fluorine-doped SnO_2 over layer, sheet resistance of $10 \Omega/\text{sq}$) using a screen printing technique. The thickness of the TiO_2 film was controlled by selection of screen mesh size and repetition of printing. The film was dried in air at 120°C for 30 min and calcined at 500°C for

30 min under flowing oxygen before cooling to room temperature. The heated electrodes were impregnated with a 0.05 M titanium tetrachloride solution in a water-saturated desiccator at 70 °C for 30 min and fired again to give a ca. 10 μm thick mesoscopic TiO₂ film. The TiO₂ electrode was stained by immersing it into a dye solution containing 300 μM dye sensitizers (ethanol/dichloromethane 3.5:1.5) for 24 h at room temperature. Then the sensitized-electrode was rinsed with dry ethanol and dried by a dry air flow. Pt catalyst was deposited on the FTO glass by coating with a drop of H₂PtCl₆ solution (40 mM in ethanol) with the heat treatment at 395 °C for 15 min to give photoanode. The dye-covered TiO₂ electrode and Pt-counter electrode were assembled into a sandwich type cell using a hot-melt Surlyn film. The electrolyte consisted of 0.6 M 1,2-dimethyl-3-*n*-propylimidazolium iodide (DMPIml), 0.1 M LiI, 0.05 M I₂, and 0.5 M *tert*-butylpyridine in acetonitrile was introduced through a hole drilled in the back of the counter electrode. Finally, the hole was also sealed with Surlyn film.

The photocurrent–voltage (*J*–*V*) characteristics of solar cells were carried out using a Keithley 2400 digital source meter controlled by a computer and a standard AM 1.5 solar simulator-Oriel 91160-1000 (300 W) SOLAR SIMULATOR 2×2 BEAM. The active electrode area was 0.16 cm². The action spectra of monochromatic incident photon-to-current conversion efficiency (IPCE) for solar cells were performed by using a commercial setup (QTest Station 2000 IPCE Measurement System, CROWNTECH, USA).

Electrochemical impedance spectroscopy (EIS) in the frequency range of 100 mHz to 100 kHz was performed with a PARSTAT 2273 potentiostat/galvanostat/FRA in the dark with the alternate current amplitude set at 10 mV. For the open-circuit voltage decay (OCVD) measurements, the DSSC was illuminated with a green LED (OPT Dongguan, λ_{max}=515 nm) as the light source. The illumination was turned off with a computer-controlled electronic shutter. The OCVD was recorded by an LK2005A electrochemical workstation as soon as the shutter brought a full darkness. The measurement interval of the voltage decay was 50–100 ms.

4.4. The detailed experimental procedures and characterization data

4.4.1. Synthesis of 2-bromo-4,4'-dioxidedithieno[3,2-*b*:2',3'-*d*]thiophene (2). A flask protected from light was charged with compound **1** (251 mg, 1.101 mmol) in 15 mL DMF. NBS (177 mg, 0.991 mmol) was added stepwise over 90 min at 15 °C. The mixture was stirred for 24 h at room temperature. Water (20 mL) was added to terminate the reaction and the product was extracted with CH₂Cl₂ (DCM). The combined organic layers were washed with brine and dried with anhydrous Na₂SO₄. The solvent was evaporated, and the remaining crude product was purified by column chromatography to give a yellow powder of **2** (229 mg, 75%). Mp: 224–226 °C; ¹H NMR (400 MHz, CDCl₃): δ 7.37 (d, 1H, *J*=5.1 Hz), 7.22 (s, 1H), 7.20 (d, 1H, *J*=5.1 Hz); ¹³C NMR (100 MHz, CDCl₃): δ 142.4, 142.3, 135.9, 135.5, 130.0, 122.7, 120.4, 116.5. HRMS (ESI) calcd for C₈H₃BrO₂S₃ (M+Na)⁺: 328.8371, found: 328.8372.

4.4.2. Synthesis of 2-(4-[*N,N*-bis(4-hexyloxyphenyl)amino]phenyl)-4,4'-dioxidedithieno[3,2-*b*:2',3'-*d*]thiophene (3). A solution of 4-(tributylstannyl)-*N,N*-bis((4-hexyloxy)phenyl)aniline (210 mg, 0.286 mmol) in 10 mL *p*-xylene was added to a solution of **2** (55 mg, 0.179 mmol) and Pd(PPh₃)₄ (10 mol%) in 10 mL *p*-xylene. The mixture was refluxed under nitrogen for 24 h. After cooling to room temperature, 25 mL water was added to terminate the reaction and the product was extracted with ethyl acetate. The combined organic layers were washed with brine and dried with anhydrous Na₂SO₄. The solvent was evaporated, and the remaining crude product was purified by column chromatography to give a tan oil of **3** (0.110 g, 75%). IR (neat): 3084, 1623, 1460, 1363, 1083 cm⁻¹. ¹H

NMR (400 MHz, CDCl₃): δ 7.32–7.30 (m, 3H), 7.22–7.20 (m, 2H), 7.09 (d, *J*=8.9 Hz, 4H), 6.90 (d, *J*=8.8 Hz, 2H), 6.86 (d, *J*=8.8 Hz, 4H), 3.96 (t, *J*=6.5 Hz, 4H), 1.82–1.75 (m, 4H), 1.50–1.45 (m, 4H), 1.37–1.34 (m, 8H), 0.93 (t, *J*=6.8 Hz, 6H). ¹³C NMR (100 MHz, DMSO-*d*₆): δ 156.2, 150.3, 149.6, 144.1, 142.0, 139.5, 136.5, 132.4, 132.0, 127.7, 126.9, 123.7, 120.5, 118.7, 116.0, 114.4, 68.1, 31.5, 29.2, 25.7, 22.5, 14.3. HRMS (ESI) calcd for C₃₈H₄₁NO₄S₃ (M+H)⁺: 672.2270, found: 672.2279.

4.4.3. Synthesis of 2-{2-[4-[*N,N*-bis(4-hexyloxyphenyl)amino]phenyl]-4,4'-dioxidedithieno[3,2-*b*:2',3'-*d*]thiophene-6-yl}3,4-ethylenedioxythiophene (5). Under exclusion of light, NBS (24 mg, 0.133 mmol) was added to a solution of **3** (82 mg, 0.133 mmol) in 15 mL DMF at room temperature. The mixture was stirred for 24 h before quenching with water and the product was extracted with DCM. The combined organic layers were washed with brine and dried with anhydrous Na₂SO₄. The solvent was evaporated, and the remaining crude product was purified by column chromatography to give a red powder (50 mg, 50%). The crude **4** was used for the next step without any purification. A sample of **4** (33 mg, 0.044 mmol) and 2-(tributylstannyl)-3,4-(ethylenedioxy)thiophene (34 mg, 0.066 mmol) were added to a 10 mL *p*-xylene solution of Pd(PPh₃)₄ (10 mol%). The mixture was refluxed under nitrogen for 5 h. After cooling to room temperature, 25 mL water was added to terminate the reaction and the product was extracted with ethyl acetate. The combined organic layers were washed with brine and dried with anhydrous Na₂SO₄. The solvent was evaporated, and the remaining crude product was purified by column chromatography to give a red solid of **5** (26 mg, 73%). Mp: 99–101 °C. IR (KBr): 3025, 1507, 1196, 1067 cm⁻¹. ¹H NMR (400 MHz, CDCl₃): δ 7.31 (d, *J*=8.5 Hz, 2H), 7.28 (s, 1H), 7.20 (s, 1H), 7.08 (d, *J*=8.7 Hz, 4H), 6.89 (d, *J*=8.7 Hz, 2H), 6.86 (d, *J*=8.7 Hz, 4H), 6.31 (s, 1H), 4.37–4.26 (m, 4H), 3.96 (t, *J*=6.5 Hz, 4H), 1.81–1.74 (m, 4H), 1.48–1.43 (m, 4H), 1.36–1.34 (m, 8H), 0.93 (t, *J*=6.5 Hz, 6H). ¹³C NMR (100 MHz, CDCl₃): δ 156.1, 149.9, 149.7, 142.8, 141.9, 141.9, 139.7, 139.5, 138.9, 133.2, 132.6, 127.2, 126.4, 123.9, 119.4, 115.4, 114.3, 113.5, 110.7, 98.9, 68.3, 65.2, 64.5, 31.6, 29.3, 25.8, 22.6, 14.0. HRMS (ESI) calcd for C₄₄H₄₅NO₆S₄ (M+H)⁺: 812.2202, found: 812.2190.

4.4.4. Synthesis of 2-{2-[4-[*N,N*-bis(4-hexyloxyphenyl)amino]phenyl]-4,4'-dioxidedithieno[3,2-*b*:2',3'-*d*]thiophene-6-yl}3,4-ethylenedioxythiophene-5-carbaldehyde (6). POCl₃ (0.5 mL, 5.479 mmol) was added dropwise to dry DMF (8 mL) at 0 °C. The reaction mixture was kept at 0 °C for 1 h and compound **5** (50 mg, 0.062 mmol) was added. After cooling to room temperature, the mixture was stirred for 1 h. The pH was adjusted to 10 with 1 M NaOH and the product was extracted with DCM. The combined organic layers were washed with saturated NH₄Cl and dried with anhydrous Na₂SO₄. The solvent was evaporated, and the remaining crude product was purified by column chromatography to give a violet powder of **6** (0.039 g, 55%). Mp: 245–247 °C. IR (KBr): 1640, 1505, 1197, 1078 cm⁻¹. ¹H NMR (400 MHz, CDCl₃): δ 9.92 (s, 1H), 7.50 (s, 1H), 7.31 (d, *J*=8.6 Hz, 2H), 7.21 (s, 1H), 7.08 (d, *J*=8.8 Hz, 4H), 6.89–6.84 (m, 6H), 4.46 (s, 4H), 3.95 (t, *J*=6.4 Hz, 4H), 1.81–1.75 (m, 4H), 1.48–1.43 (m, 4H), 1.36–1.34 (m, 8H), 0.93 (t, *J*=6.5 Hz, 6H). ¹³C NMR (100 MHz, CDCl₃): δ 179.2, 156.2, 151.3, 149.9, 148.1, 143.6, 142.0, 139.6, 138.1, 137.4, 136.0, 131.5, 127.3, 126.4, 123.5, 120.6, 119.1, 115.5, 113.4, 68.3, 65.2, 65.1, 31.6, 29.3, 25.8, 22.6, 14.0. HRMS (ESI) calcd for C₄₅H₄₅NO₇S₄ (M+H)⁺: 840.2152, found: 840.2142.

4.4.5. Synthesis of 2-(3,4-ethylenedioxythiophene)-dithieno[3,2-*b*:2',3'-*d*]thiophene (8). Compound **8** was synthesized according to the same procedure of **5**, giving a light yellow needle-like solid of **8** (192 mg, 35%). Mp: 167–169 °C. ¹H NMR (400 MHz, CDCl₃): δ 7.39 (s, 1H), 7.31 (d, *J*=5.2 Hz, 1H), 7.25 (d, *J*=5.2 Hz, 1H), 6.26 (s, 1H),

4.34–4.22 (m, 4H), ^{13}C NMR (100 MHz, DMSO- d_6): 142.2, 141.9, 141.6, 138.7, 135.3, 130.5, 128.7, 127.8, 121.9, 116.6, 111.1, 98.6, 65.66, 64.8. HRMS (ESI) calcd for $\text{C}_{14}\text{H}_8\text{O}_2\text{S}_4$ ($\text{M}+\text{H}$) $^+$: 336.9450, found: 336.9483.

4.4.6. Synthesis of 2-Bromothieno-3-methyl-1,1'-dioxide[3,2-*b*]thiophene (13). A 20 mL solution of 3-chloroperbenzoic acid (75%, 0.772 g, 3.347 mmol) previously dried over magnesium sulfate was added dropwise to a solution of **12** (0.200 g, 0.862 mmol) in 20 mL of dichloromethane at 0 °C. The mixture was stirred at room temperature overnight before washing sequentially with 10% KOH, 10% NaHCO_3 , and brine. The combined organic layers were dried with anhydrous Na_2SO_4 . The solvent was evaporated, and the remaining crude product was purified by column chromatography to give a gray needle-like solid of **13** (0.125 g, 55%). Mp: 183–185 °C. IR (KBr): 3098, 1348, 1301, 1131 cm^{-1} . ^1H NMR (400 MHz, CDCl_3): δ 7.51 (d, $J=5.0$ Hz, 1H), 7.29 (d, $J=5.0$ Hz, 1H), 2.21 (s, 3H). ^{13}C NMR (100 MHz, CDCl_3): δ 144.0, 137.0, 133.7, 130.6, 120.9, 119.0, 14.4. HRMS (ESI) calcd for $\text{C}_7\text{H}_5\text{BrO}_2\text{S}_2$ ($\text{M}+\text{H}$) $^+$: 264.8987, found: 264.8987.

4.4.7. Synthesis of 2-(3,4-ethylenedioxythiophene)-3-methyl-1,1'-dioxide[3,2-*b*]thiophene (14). Compound **14** was synthesized according to the same procedure of **8**, giving yellow solid of **14** in 31% yield. Mp: 223–225 °C. IR (KBr): 3117, 2917, 1488, 1429, 1148, 1069 cm^{-1} . ^1H NMR (400 MHz, CDCl_3): δ 7.42 (d, $J=5.0$ Hz, 1H), 7.27 (d, $J=5.0$ Hz, 1H), 6.58 (s, 1H), 4.29–4.24 (m, 4H), 2.23 (s, 3H). ^{13}C NMR (100 MHz, CDCl_3): δ 145.5, 141.8, 141.6, 137.6, 132.8, 131.0, 130.5, 120.5, 103.6, 102.0, 65.0, 64.4, 29.7, 14.8. HRMS (ESI) calcd for $\text{C}_{13}\text{H}_{10}\text{O}_4\text{S}_3$ ($\text{M}+\text{H}$) $^+$: 326.9814, found: 326.9818.

4.4.8. Synthesis of 2-(3,4-ethylenedioxythiophene)-3-methyl-[3,2-*b*]thiophene (18). Compound **18** was synthesized according to the same procedure of **8**, giving light yellow liquid of **18** in 30% yield. IR (KBr): 2920, 1489, 1363, 1072 cm^{-1} . ^1H NMR (400 MHz, CDCl_3): δ 7.33 (d, $J=5.2$ Hz, 1H), 7.21 (d, $J=5.2$ Hz, 1H), 6.40 (s, 1H), 4.28–4.22 (m, 4H), 2.23 (s, 3H). ^{13}C NMR (100 MHz, CDCl_3): δ 141.9, 141.7, 138.4, 137.1, 129.4, 127.3, 126.2, 120.0, 110.9, 99.6, 64.9, 64.5, 14.7. HRMS (ESI) calcd for $\text{C}_{13}\text{H}_{10}\text{O}_2\text{S}_3$ ($\text{M}+\text{H}$) $^+$: 294.9916, found: 294.9916.

4.4.9. Synthesis of 2-(dithieno[3,2-*b*:2',3'-*d*]thiophen)-(3,4-ethylenedioxythiophene)-5-carbaldehyde (9). Compound **9** was synthesized according to the same procedure of **6**, giving a yellow solid of **9** (324 mg, 89%). Mp: 201–203 °C. IR (KBr): 3073, 1636, 1458, 1210, 1085 cm^{-1} . ^1H NMR (400 MHz, CDCl_3): δ 9.92 (s, 1H), 7.64 (s, 1H), 7.42 (d, $J=5.2$ Hz, 1H), 7.30 (d, $J=5.2$ Hz, 1H), 4.74–4.44 (m, 4H). ^{13}C NMR (100 MHz, CDCl_3): δ 179.3, 148.5, 142.5, 141.8, 137.1, 133.8, 131.7, 130.8, 127.0, 123.3, 120.9, 119.2, 115.0, 65.3, 64.9. HRMS (ESI) calcd for $\text{C}_{15}\text{H}_8\text{O}_3\text{S}_4$ ($\text{M}+\text{H}$) $^+$: 364.9429, found: 364.9434.

4.4.10. Synthesis of 2-(3-methyl-1,1'-dioxide[3,2-*b*]thiophene)-(3,4-ethylenedioxythiophene)-5-carbaldehyde (15). Compound **15** was synthesized according to the same procedure of **6**, giving brown solid of **15** in 75% yield. Mp: 254–256 °C. IR (KBr): 3085, 2939, 1638, 1445, 1302, 1085 cm^{-1} . ^1H NMR (400 MHz, CDCl_3): δ 9.97 (s, 1H), 7.50 (d, $J=5.0$ Hz, 1H), 7.30 (d, $J=5.0$ Hz, 1H), 4.45–4.37 (m, 4H), 2.28 (s, 3H). ^{13}C NMR (100 MHz, CDCl_3): δ 145.5, 141.8, 141.6, 137.6, 132.8, 131.0, 130.5, 120.5, 103.6, 102.0, 65.0, 64.4, 29.7, 14.8. HRMS (ESI) calcd for $\text{C}_{14}\text{H}_{10}\text{O}_5\text{S}_3$ ($\text{M}+\text{H}$) $^+$: 354.9763, found: 354.9768.

4.4.11. Synthesis of 2-(3-methyl-[3,2-*b*]thiophene)-(3,4-ethylenedioxythiophene)-5-carbaldehyde (19). Compound **19** was synthesized according to the same procedure of **6**, giving yellow solid of **19** in 80% yield. Mp: 236–238 °C. IR (KBr): 3083, 2962, 1626,

1510, 1279, 1087 cm^{-1} . ^1H NMR (400 MHz, CDCl_3): δ 9.95 (s, 1H), 7.43 (d, $J=5.2$ Hz, 1H), 7.25 (d, $J=5.2$ Hz, 1H), 4.45–4.40 (m, 4H), 2.54 (s, 3H). ^{13}C NMR (100 MHz, CDCl_3): δ 179.5, 148.3, 142.4, 138.5, 137.4, 129.1, 128.3, 127.9, 122.9, 119.9, 116.8, 65.2, 64.7, 15.5. HRMS (ESI) calcd for $\text{C}_{14}\text{H}_{10}\text{O}_3\text{S}_3$ ($\text{M}+\text{H}$) $^+$: 322.9865, found: 322.9868.

4.4.12. Synthesis of 2-{2-[4-[*N,N*-bis(4-hexyloxyphenyl)amino]phenyl]dithieno[3,2-*b*:2',3'-*d*]thiophene-6-yl}3,4-ethylenedioxythiophene-5-carbaldehyde (11). Compound **11** was synthesized according to the same procedure of **3**, giving a red solid of **11** (174 mg, 36%). IR (KBr): 2927, 2855, 1640, 1475, 1079 cm^{-1} . ^1H NMR (400 MHz, DMSO- d_6): δ 9.86 (s, 1H), 7.96 (s, 1H), 7.77 (s, 1H), 7.53 (d, $J=8.7$ Hz, 2H), 7.07 (d, $J=8.7$ Hz, 4H), 6.94 (d, $J=8.9$ Hz, 4H), 6.80 (d, $J=8.9$ Hz, 2H), 4.40 (s, 4H), 3.96 (t, $J=6.4$ Hz, 4H), 1.73–1.69 (m, 4H), 1.42–1.24 (m, 12H), 0.92–0.87 (m, 6H). ^{13}C NMR (100 MHz, CDCl_3): δ 179.1, 155.8, 148.9, 148.5, 146.8, 143.4, 140.7, 140.1, 136.9, 132.1, 130.9, 130.0, 128.8, 126.9, 126.3, 125.8, 123.6, 119.9, 119.1, 115.2, 114.8, 68.3, 65.3, 64.8, 31.6, 29.3, 25.7, 22.6, 14.0. HRMS (ESI) calcd for $\text{C}_{45}\text{H}_{45}\text{NO}_5\text{S}_4$ ($\text{M}+\text{H}$) $^+$: 808.2253, found: 808.2256.

4.4.13. Synthesis of 2-{2-[4-[*N,N*-bis(4-hexyloxyphenyl)amino]phenyl]6-methyl-1,1'-dioxide[3,2-*b*]thiophen-5-yl}3,4-ethylenedioxythiophene-5-carbaldehyde (17). Compound **17** was synthesized according to the same procedure of **3**, giving purple solid of **17** in 35% yield. IR (KBr): 2928, 2855, 1640, 1475, 1079 cm^{-1} . ^1H NMR (400 MHz, CDCl_3): δ 9.96 (s, 1H), 7.34 (d, $J=8.8$ Hz, 2H), 7.28 (s, 1H), 7.09 (d, $J=8.9$ Hz, 4H), 6.90 (d, $J=8.8$ Hz, 2H), 6.86 (d, $J=8.9$ Hz, 4H), 4.43–4.38 (m, 4H), 3.96 (t, $J=6.5$ Hz, 4H), 2.27 (s, 3H), 1.80–1.74 (m, 4H), 1.48–1.34 (m, 12H), 0.93–0.90 (m, 6H). ^{13}C NMR (100 MHz, CDCl_3): δ 156.1, 150.5, 149.8, 144.0, 142.0, 139.7, 136.9, 131.9, 128.7, 127.2, 126.5, 123.7, 120.2, 119.3, 115.4, 113.5, 68.3, 31.6, 29.3, 26.9, 25.7, 22.6, 14.0. HRMS (ESI) calcd for $\text{C}_{44}\text{H}_{47}\text{NO}_7\text{S}_3$ ($\text{M}+\text{H}$) $^+$: 798.2587, found: 798.2599.

4.4.14. Synthesis of 2-{2-[4-[*N,N*-bis(4-hexyloxyphenyl)amino]phenyl]6-methyl[3,2-*b*]thiophen-5-yl}3,4-ethylenedioxythiophene-5-carbaldehyde (21). Compound **20** was synthesized according to the same procedure of **10**. The crude **20** was used for the next step without any purification. Compound **21** was synthesized according to the same procedure of **11**, giving red oily liquid of **21** in 32% yield. IR (KBr): 2927, 2854, 1599, 1507, 1301, 1032 cm^{-1} . ^1H NMR (400 MHz, CDCl_3): δ 9.92 (s, 1H), 7.41 (d, $J=8.8$ Hz, 2H), 7.28 (s, 1H), 7.07 (d, $J=8.9$ Hz, 4H), 6.92 (d, $J=8.8$ Hz, 2H), 6.84 (d, $J=8.9$ Hz, 4H), 4.41–4.38 (m, 4H), 3.94 (t, $J=6.5$ Hz, 4H), 2.51 (s, 3H), 1.81–1.74 (m, 4H), 1.48–1.42 (m, 4H), 1.36–1.32 (m, 8H), 0.93 (t, $J=7.0$ Hz, 6H). ^{13}C NMR (100 MHz, CDCl_3): δ 179.4, 155.8, 148.3, 147.6, 140.5, 140.2, 139.7, 137.1, 129.2, 126.9, 126.4, 123.5, 120.0, 116.3, 115.4, 113.9, 68.3, 65.2, 64.7, 31.6, 29.3, 26.7, 25.8, 22.6, 14.1. HRMS (ESI) calcd for $\text{C}_{44}\text{H}_{47}\text{NO}_5\text{S}_3$ ($\text{M}+\text{H}$) $^+$: 766.2689, found: 766.2688.

4.4.15. Synthesis of 3-{2-[2-[4-[*N,N*-bis(4-hexyloxyphenyl)amino]phenyl]-4,4'-dioxidedithieno[3,2-*b*:2',3'-*d*]thiophene-6-yl]}3,4-ethylenedioxythiophene-2-yl}-2-cyanoacrylic acid (XS35). To a stirred solution of compound **6** (100 mg, 0.119 mmol) and cyanoacetic acid (30 mg, 0.357 mmol) in a 1:1 mixture of chloroform and acetic acid was added catalytic amount of piperidine (50 μL). The reaction mixture was refluxed for 12 h and then the solvent was removed in vacuo. The resulting solid was dissolved in DCM and sequentially washed with brine and dried with anhydrous Na_2SO_4 . The solvent was evaporated, and the remaining crude product was purified by column chromatography to give a purple solid of **XS35** (83%). Mp: >300 °C. IR (KBr): 3400, 2930, 2861, 1600, 1510, 1320, 823 cm^{-1} . ^1H NMR (400 MHz, DMSO- d_6): δ 8.83 (s, 1H), 8.05 (s, 1H), 7.71 (s, 2H), 7.45 (s, 2H), 7.09–6.92 (m, 7H), 6.70 (s, 2H), 4.51–4.48 (m, 4H), 4.00–3.93 (m, 4H), 1.58–1.50 (m, 4H), 1.45–1.26 (m, 12H), 0.91–0.82 (m, 6H). ^{13}C NMR (100 MHz, pyridine- d_5): δ 158.5, 156.5,

150.9, 149.0, 143.7, 142.3, 140.1, 138.3, 135.9, 132.1, 127.5, 126.8, 126.7, 124.3, 124.2, 123.8, 122.8, 120.0, 119.4, 117.8, 115.9, 114.2, 68.3, 65.6, 65.4, 31.5, 29.4, 25.8, 22.6, 13.9. HRMS (ESI) calcd for $C_{48}H_{46}N_2O_8S_4$ (M+H)⁺: 907.2210, found: 907.2226.

4.4.16. Synthesis of 3-[2-[2-[4-[N,N-bis(4-hexyloxyphenyl)amino]phenyl]dithieno[3,2-b:2',3'-d]thiophene-6-yl]3,4-ethylenedioxythiophene-2-yl]-2-cyanoacrylic acid (XS36). Compound **XS36** was synthesized according to the same procedure of **XS35**, giving a red oily liquid of **XS36** in 87% yield. Mp: >300 °C. IR (KBr): 3420, 2930, 2860, 1602, 1513, 1381, 1070 cm⁻¹. ¹H NMR (400 MHz, DMSO-d₆): δ 8.04 (s, 1H), 7.75 (s, 1H), 7.69 (s, 1H), 7.48 (d, J=8.5 Hz, 2H), 7.04 (d, J=8.8 Hz, 4H), 6.92 (d, J=8.8 Hz, 4H), 6.78 (d, J=8.5 Hz, 2H), 4.50–4.48 (m, 4H), 3.95 (t, J=6.4 Hz, 4H), 1.72–1.68 (m, 4H), 1.43–1.40 (m, 4H), 1.32–1.31 (m, 8H), 0.90–0.87 (m, 6H). ¹³C NMR (100 MHz, pyridine-d₅): δ 157.7, 151.7, 150.3, 147.6, 144.9, 142.7, 142.0, 138.7, 136.3, 135.4, 130.1, 128.8, 128.2, 128.0, 125.3, 124.2, 121.6, 117.3, 116.8, 69.8, 65.7, 65.4, 33.1, 30.9, 27.3, 24.1, 15.4. HRMS (ESI) calcd for $C_{48}H_{46}N_2O_6S_4$ (M+H)⁺: 875.2311, found: 875.2288.

4.4.17. Synthesis of 3-[2-[2-[4-[N,N-bis(4-hexyloxyphenyl)amino]phenyl]6-methyl-1,1'-dioxide[3,2-b]thiophen-5-yl]3,4-ethylenedioxythiophene-2-yl]-2-cyanoacrylic acid (XS37). Compound **XS37** was synthesized according to the same procedure of **XS35**, giving a red oily liquid of **XS37** in 86% yield. Mp: >300 °C. IR (KBr): 3421, 2931, 2865, 1611, 1512, 1243, 1071 cm⁻¹. ¹H NMR (400 MHz, DMSO-d₆): δ 8.10 (s, 1H), 7.88 (s, 1H), 7.55 (d, J=8.6 Hz, 2H), 7.08 (d, J=8.8 Hz, 4H), 6.94 (d, J=8.8 Hz, 4H), 6.74 (d, J=8.6 Hz, 2H), 4.44–4.42 (m, 4H), 3.96 (t, J=6.4 Hz, 4H), 2.26 (s, 3H), 1.72–1.69 (m, 4H), 1.41–1.31 (m, 12H), 0.90–0.87 (m, 6H). ¹³C NMR (100 MHz, pyridine-d₅): δ 158.1, 150.5, 142.8, 141.5, 141.2, 137.3, 136.3, 129.1, 128.4, 125.7, 125.3, 124.2, 120.9, 117.4, 116.3, 116.0, 69.7, 66.8, 66.5, 33.0, 31.2, 27.3, 24.1, 15.4. HRMS (ESI) calcd for $C_{47}H_{48}N_2O_8S_3$ (M+NH₄)⁺: 882.2911, found: 882.2898.

4.4.18. Synthesis of 3-[2-[2-[4-[N,N-bis(4-hexyloxyphenyl)amino]phenyl]6-methyl[3,2-b]thiophen-5-yl]3,4-ethylenedioxythiophene-2-yl]-2-cyanoacrylic acid (XS38). Compound **XS38** was synthesized according to the same procedure of **XS35**, giving a red oily liquid of **XS38** in 91% yield. Mp: >300 °C. IR (KBr): 3418, 2921, 2218, 1587, 1374, 1075 cm⁻¹. ¹H NMR (400 MHz, DMSO-d₆): δ 8.09 (s, 1H), 7.65 (s, 1H), 7.51 (d, J=8.6 Hz, 2H), 7.05 (d, J=8.8 Hz, 4H), 6.92 (d, J=8.8 Hz, 4H), 6.78 (d, J=8.6 Hz, 2H), 4.45–4.43 (m, 4H), 3.95 (t, J=6.4 Hz, 4H), 2.50 (s, 3H), 1.74–1.67 (m, 4H), 1.43–1.31 (m, 12H), 0.90–0.87 (m, 6H). ¹³C NMR (100 MHz, pyridine-d₅): δ 157.7, 150.6, 150.5, 148.5, 142.1, 142.0, 141.3, 139.1, 137.3, 136.3, 129.9, 128.7, 128.2, 128.1, 125.3, 124.2, 121.8, 117.3, 116.1, 113.2, 69.8, 67.1, 66.4, 33.0, 30.9, 27.3, 24.1, 16.7, 15.4. HRMS (ESI) calcd for $C_{47}H_{48}N_2O_6S_3$ (M+H)⁺: 833.2747, found: 833.2718.

Acknowledgements

We are grateful to the National Natural Science Foundation of China (21003096, 21072152) and the Tianjin Natural Science Foundation (09JCZDJ24400) for financial supports.

References and notes

- O'Regan, B.; Grätzel, M. *Nature* **1991**, *353*, 737.
- (a) Gao, F.; Wang, Y.; Shi, D.; Zhang, J.; Wang, M.; Jing, X.; Humphry-Baker, R.; Wang, P.; Zakeeruddin, S. M.; Grätzel, M. *J. Am. Chem. Soc.* **2008**, *130*, 10720; (b) Nazeeruddin, M. K.; De Angelis, F.; Fantacci, S.; Selloni, A.; Viscardi, G.; Liska, P.; Ito, S.; Takeru, B.; Grätzel, M. *J. Am. Chem. Soc.* **2005**, *127*, 16835.
- (a) Hagfeldt, A.; Boschloo, G.; Sun, L.; Kloo, L.; Pettersson, H. *Chem. Rev.* **2010**, *110*, 6595; (b) Mishra, A.; Fischer, M. K. R.; Bauerle, P. *Angew. Chem., Int. Ed.* **2009**, *48*, 2474.
- Zhou, H.; Xue, P.; Zhang, Y.; Zhao, X.; Jia, J.; Zhang, X.; Liu, X.; Lu, R. *Tetrahedron* **2011**, *67*, 8477.
- Zhang, L.; Liu, Y.; Wang, Z.; Liang, M.; Sun, Z.; Xue, S. *Tetrahedron* **2012**, *68*, 552.
- Higashijima, S.; Miura, H.; Fujita, T.; Kubota, Y.; Funabiki, K.; Yoshida, T.; Matsui, M. *Tetrahedron* **2011**, *67*, 6289.
- Chang, Y. J.; Chow, T. J. *Tetrahedron* **2009**, *65*, 9626.
- Chou, H.-H.; Hsu, C.-Y.; Hsu, Y.-C.; Lin, Y.-S.; Lin, J. T.; Tsai, C. *Tetrahedron* **2012**, *68*, 767.
- Sahu, D.; Padhy, H.; Patra, D.; Yin, J.-F.; Hsu, Y.-C.; Lin, J.-T.; Lu, K.-L.; Wei, K.-H.; Lin, H.-C. *Tetrahedron* **2011**, *67*, 303.
- Choi, H.; Lee, J. K.; Song, K.; Kang, S. O.; Ko, J. *Tetrahedron* **2007**, *63*, 3115.
- Hara, K.; Sayama, K.; Ohga, Y.; Shinpo, A.; Suga, S.; Arakawa, H. *Chem. Commun.* **2001**, 569.
- Wang, Z. S.; Cui, Y.; Hara, K.; Dan-Oh, Y.; Kasada, C.; Shinpo, A. *Adv. Mater.* **2007**, *19*, 1138.
- Kuang, D.; Uchida, S.; Humphry-Baker, R.; Zakeeruddin, S. M.; Grätzel, M. *Angew. Chem., Int. Ed.* **2008**, *47*, 1923.
- Thomas, K. R. J.; Hsu, Y. C.; Lin, J. T.; Lee, K. M.; Ho, K. C.; Lai, C. H.; Cheng, Y. M.; Chou, P. T. *Chem. Mater.* **2008**, *20*, 1830.
- Wu, W.; Yang, J.; Hua, J.; Tang, J.; Zhang, L.; Long, Y.; Tian, H. J. *Mater. Chem.* **2010**, *20*, 1772.
- He, J.; Wu, W.; Hua, J.; Jiang, Y.; Qu, S.; Li, J.; Long, Y.; Tian, H. J. *Mater. Chem.* **2011**, *21*, 6054.
- Hagberg, D. P.; Yum, J. H.; Lee, H.; De Angelis, F.; Marinado, T.; Karlsson, K. M.; Humphry-Baker, R.; Sun, L. C.; Hagfeldt, A.; Grätzel, M.; Nazeeruddin, M. K. J. *Am. Chem. Soc.* **2008**, *130*, 6259.
- Lu, M.; Liang, M.; Han, H.; Sun, Z.; Xue, S. *J. Phys. Chem. C* **2011**, *115*, 274.
- Liang, M.; Lu, M.; Wang, Q.; Chen, W.; Han, H.; Sun, Z.; Xue, S. *J. Power Sources* **2011**, *196*, 1657.
- Hao, X.; Liang, M.; Cheng, X.; Pian, X.; Sun, Z.; Xue, S. *Org. Lett.* **2011**, *13*, 5424.
- Liang, Y.; Peng, B.; Liang, J.; Tao, Z.; Chen, J. *Org. Lett.* **2010**, *12*, 1204.
- Paek, S.; Choi, H.; Choi, H.; Lee, C.; Kang, M.; Song, K.; Nazeeruddin, M.; Ko, J. *J. Phys. Chem. C* **2010**, *114*, 14646.
- Choi, H.; Baik, C.; Kang, S. O.; Ko, J.; Kang, M. S.; Nazeeruddin, M. K.; Grätzel, M. *Angew. Chem., Int. Ed.* **2008**, *47*, 327.
- Numata, Y.; Ashraf, I.; Shirai, Y.; Han, L. *Chem. Commun.* **2011**, 6159.
- Zhu, W. H.; Wu, Y. Z.; Wang, S. T.; Li, W. Q.; Li, X.; Chen, J. A.; Wang, Z.-S.; Tian, H. *Adv. Funct. Mater.* **2011**, *21*, 756.
- Zeng, W.; Cao, Y.; Bai, Y.; Wang, Y.; Shi, Y.; Zhang, M.; Wang, F.; Pan, C.; Wang, P. *Chem. Mater.* **2010**, *22*, 1915.
- Im, H.; Kim, S.; Park, C.; Jang, S.; Kim, C.; Kim, K.; Park, N.; Kim, C. *Chem. Commun.* **2010**, 1335.
- Ito, S.; Miura, H.; Uchida, S.; Takata, M.; Sumioka, K.; Liska, P.; Comte, P.; Pechy, P.; Grätzel, M. *Chem. Commun.* **2008**, 5194.
- Chen, D.; Hsu, Y.; Hsu, H.; Chen, B.; Lee, Y.; Fu, H.; Chung, M.; Liu, S.; Chen, H.; Chou, P. *Chem. Commun.* **2010**, 5256.
- Zhang, G. L.; Bala, H.; Cheng, Y. M.; Shi, D.; Lv, X. J.; Yu, Q. J.; Wang, P. *Chem. Commun.* **2009**, 2198.
- Qin, H.; Wenger, S.; Xu, M.; Gao, F.; Jing, X.; Wang, P.; Zakeeruddin, S. M.; Grätzel, M. *J. Am. Chem. Soc.* **2008**, *130*, 9202.
- Kwon, T.; Armel, V.; Nattestad, A.; MacFarlane, D.; Bach, U.; Lind, S.; Gordon, K.; Tang, W.; Jones, D.; Holmes, A. *J. Org. Chem.* **2011**, *76*, 4088.
- Cheng, X.; Sun, S.; Liang, M.; Shi, Y.; Sun, Z.; Xue, S. *Dyes Pigments* **2012**, *92*, 1292.
- Zhang, Z. G.; Wang, J. Z. *J. Mater. Chem.* **2012**, *22*, 4178.
- Liu, C.; Li, Y. J.; Li, C. H.; Li, W. W.; Zhou, C. J.; Liu, H. B.; Bo, Z. S.; Li, Y. L. *J. Phys. Chem. C* **2009**, *113*, 21970.
- Liu, C.; Xiao, S. Q.; Shu, X. P.; Li, Y. J.; Xu, L.; Liu, T. F.; Yu, Y. W.; Zhang, L.; Liu, H. B.; Li, Y. L. *ACS Appl. Mater. Interfaces* **2012**, *4*, 1065.
- Allared, F.; Hellberg, J.; Remonen, T. *Tetrahedron Lett.* **2002**, *43*, 1553.
- Zhang, X.; Köhler, M.; Matzger, A. *J. Macromolecules* **2004**, *37*, 6306.
- Miguel, L. S.; Matzger, A. *J. Org. Chem.* **2008**, *73*, 7882.
- Sotgiu, G.; Zambianchi, M.; Barbarella, G.; Aruffo, F.; Cipriani, F.; Ventola, A. *J. Org. Chem.* **2003**, *68*, 1512.
- Zhou, D.; Cai, N.; Long, H.; Zhang, M.; Wang, Y.; Wang, P. *J. Phys. Chem. C* **2011**, *115*, 3163.
- Lin, L.-Y.; Tsai, C.-H.; Wong, K.-T.; Huang, T.-W.; Wu, C.-C.; Chou, S.-H.; Lin, F.; Chen, S.-H.; Tsai, A.-I. *J. Mater. Chem.* **2011**, *21*, 5950.
- Hagfeldt, A.; Grätzel, M. *Chem. Rev.* **1995**, *95*, 49.
- Li, R. Z.; Lv, X. J.; Shi, D.; Zhou, D. F.; Cheng, Y. M.; Zhang, G. L.; Wang, P. *J. Phys. Chem. C* **2009**, *113*, 7469.
- Frisch, M. J.; Trucks, G. W.; Schlegel, H. B.; Scuseria, G. E.; Robb, M. A.; Cheeseman, J. R.; Montgomery, J. A., Jr.; Vreven, T.; Kudin, K. N.; Burant, J. C.; Millam, J. M.; Iyengar, S. S.; Tomasi, J.; Barone, V.; Mennucci, B.; Cossi, M.; Scalmani, G.; Rega, N.; Petersson, G. A.; Nakatsuji, H.; Hada, M.; Ehara, M.; Toyota, K.; Fukuda, R.; Hasegawa, J.; Ishida, M.; Nakajima, T.; Honda, Y.; Kitao, O.; Nakai, H.; Klene, M.; Li, X.; Knox, J. E.; Hratchian, H. P.; Cross, J. B.; Bakken, V.; Adamo, C.; Jaramillo, J.; Gomperts, R.; Stratmann, R. E.; Yazyev, O.; Austin, A. J.; Cammi, R.; Pomelli, C.; Ochterski, J. W.; Ayala, P. Y.; Morokuma, K.; Voth, G. A.; Salvador, P.; Dannenberg, J. J.; Zakrzewski, V. G.; Dapprich, S.; Daniels, A. D.; Strain, M. C.; Farkas, O.; Malick, D. K.; Rabuck, A. D.; Raghavachari, K.; Foresman, J. B.; Ortiz, J. V.; Cui, Q.; Baboul, A. G.; Clifford, S.; Cioslowski, J.; Stefanov, B. B.; Liu, G.; Liashenko, A.; Piskorz, P.; Komaromi, I.; Martin, R. L.; Fox, D. J.; Keith, T.; Al-Laham, M. A.; Peng, C. Y.; Nanayakkara, A.; Challacombe, M.; Gill, P. M. W.; Johnson, B.; Chen, W.; Wong, M. W.; Gonzalez, C.; Pople, J. A. *Gaussian 03, Revision C.01*; Gaussian: Wallingford, CT, 2003.

46. Marinado, T.; Nonomura, K.; Nissfolk, J.; Karlsson, M. K.; Hagberg, D. P.; Sun, L.; Mori, S.; Hagfeldt, A. *Langmuir* **2010**, *26*, 2592.
47. (a) Li, J.-Y.; Chen, C.-Y.; Chen, J.-G.; Tan, C.-J.; Lee, K.-M.; Wu, S.-J.; Tung, Y.-L.; Tsai, H.-H.; Ho, K.-C.; Wu, C.-G. *J. Mater. Chem.* **2010**, *20*, 7158; (b) Kopidakis, N.; Benkstein, K. D.; van de Lagemaat, J.; Frank, A. J. *J. Phys. Chem. B* **2003**, *107*, 11307.
48. Kozma, E.; Concina, I.; Braga, A.; Borgese, L.; Depero, L. E.; Vomiero, A.; Sberveglieri, G.; Catellani, M. *J. Mater. Chem.* **2011**, *21*, 13785.
49. Boschloo, G.; Häggman, L.; Hagfeldt, A. *J. Phys. Chem. B* **2006**, *110*, 13144.
50. Pavlishchuk, V. V.; Addison, A. W. *Inorg. Chim. Acta* **2000**, *298*, 97.
51. Liang, M.; Wang, Z.-Y.; Zhang, L.; Han, H.-Y.; Sun, Z.; Xue, S. *Renew. Energy* **2011**, *36*, 2711.